ELEMENTA
Science of the Anthropocene

Impact of marine mercury cycling on coastal atmospheric mercury concentrations in the North- and Baltic Sea region

Johannes Bieser[1,2*] • Corinna Schrum[1,3]

[1]Helmholtz-Zentrum Geesthacht, Institute of Coastal Research, Geesthacht, Germany
[2]National Aeronautics and Space Research Center (DRL), Oberpfaffenhofen, Weßling, Germany
[3]University of Bergen, Geophysical Institute, Bergen, Norway
*johannes.bieser@hzg.de

Abstract

The cycling of mercury between ocean and atmosphere is an important part of the global Hg cycle. Here we study the regional contribution of the air-sea exchange in the North- and Baltic Sea region. We use a newly developed coupled regional chemistry transport modeling (CTM) system to determine the flux between atmosphere and ocean based on the meteorological model COSMO-CLM, the ocean-ecosystem model ECOSMO, the atmospheric CTM CMAQ and a newly developed module for mercury partitioning and speciation in the ocean (MECOSMO). The model was evaluated using atmospheric observations of gaseous elemental mercury (GEM), surface concentrations of dissolved gaseous mercury (DGM), and air-sea flux (ASF) calculations based on observations made on seven cruises in the western and central Baltic Sea and three cruises in the North Sea performed between 1991 and 2006. It was shown that the model is in good agreement with observations: DGM (Normalized Mean Bias NMB=-0.27 N=413), ASF (NMB=-0.32, N=413), GEM (NMB=0.07, N=2359). Generally, the model was able to reproduce the seasonal DGM cycle with the best agreement during winter and autumn (NMB_{Winter}=-0.26, NMB_{Spring}=-0.41, NMB_{Summer}=-0.29, NMB_{Autumn}=-0.03). The modelled mercury evasion from the Baltic Sea ranged from 3400 to 4000 kg/a for the simulation period 1994–2007 which is on the lower end of previous estimates. Modelled atmospheric deposition, river inflow and air-sea exchange lead to an annual net Hg accumulation in the Baltic Sea of 500 to 1000 kg/a. For the North Sea the model calculates an annual mercury flux into the atmosphere between 5700 and 6000 kg/a.

The mercury flux from the ocean influenced coastal atmospheric mercury concentrations. Running CMAQ coupled with the ocean model lead to better agreement with GEM observations. Directly at the coast GEM concentrations could be increased by up to 10% on annual average and observed peaks could be reproduced much better. At stations 100km downwind the impact was still observable but reduced to 1–3%.

Domain Editor-in-Chief
Joel D. Blum, University of Michigan

Guest Editor
Anne Soerensen, Stockholm University

Knowledge Domains
Atmospheric Science
Earth & Environmental Science
Ocean Science

Article Type
Research Article

Part of an *Elementa* Special Feature
Monitoring, measuring and modeling atmospheric mercury and air-surface exchange – are we making progress?

Received: November 5, 2015
Accepted: May 18, 2016
Published: June 29, 2016

1. Introduction

Mercury is a toxic substance that poses a severe risk to human life and ecosystems. Because of its global nature, monitoring and reduction of mercury pollution has been a focus of several international conventions, such as the UN-ECE Convention on Long-Range Transport of Atmospheric Pollution (LRTAP) (ECE, 2010), the UNEP global mercury partnership (UNEP, 2013a), and the Minamata Convention on mercury (UNEP, 2013b).

The majority of mercury on Earth is stored in deep mineral reservoirs ($3x10^8$ Gg). The second largest reservoir of mercury is the ocean with about 350 Gg (UNEP, 2013c). Historically, ocean, atmosphere, and biosphere were in a quasi steady state and the only source for additional mercury was volcanic activity, which is estimated to emit on average 90 Mg per annum (Pirrone et al., 2010). Because of mining activities and the extraction and burning of fossil fuels, mercury emissions into the atmosphere have increased dramatically over the past century (Horowitz et al., 2014). Amos et al. (2013) estimated that, compared to pre-industrial

times, the mercury burden has increased by a factor of 7.5 in the atmosphere and a factor of 5.5 in the surface ocean. In 2008, the estimated annual anthropogenic emissions of mercury from deep mineral reservoirs were 2000 Mg while emissions from the ocean (which include re-emissions of previous anthropogenic emissions) were estimated in the range of 2500 to 4000 Mg. This shows that the ocean is a major source for atmospheric mercury, even larger than the primary anthropogenic emissions. With the implementation of the Minamata Convention, future anthropogenic mercury emissions are expected to decline compared to today (Pacyna et al., 2006a). This will probably have a strong impact on the air-sea exchange. With decreasing atmospheric Hg concentration, legacy emissions driven by past deposition into the ocean might increase and lead to an even stronger influence of the ocean on the global mercury cycle.

In the environment, mercury is constantly exchanged between ocean, atmosphere, lithosphere, and biosphere. Therefore, in order to understand the global fate of mercury, it is important to take into account all environmental compartments. By means of Monte Carlo simulation, Qureshi (2011) found that the chemical reactions in the surface ocean and the air-sea exchange are two of the largest sources of uncertainty in global mercury models. This makes the ocean a reservoir of high interest for model studies to better understand the global cycle of mercury and its transport pathways.

Here we aim to study the role of the ocean and the atmosphere-ocean interactions in the regional system of the North and Baltic Sea. For this study we coupled the Eulerian regional atmospheric chemistry transport model (CTM) CMAQ with an ocean coupled hydrodynamic bio-geochemical model and expanded this with a model for marine mercury cycling, resolving transport, sedimentation and re-suspension, partitioning, and chemical speciation of mercury to determine the mercury flux between the two compartments in the North and Baltic Sea region. Here, we investigate the capability of the CTM to reproduce elemental mercury concentrations in the atmosphere and the ocean and finally the air-sea flux itself. The mercury flux from the Baltic has been estimated in the past based on a limited amount of observations (Kuss and Schneider, 2007). We compare modelled air-sea fluxes and their spatial and temporal variability with observations and investigate the influence of the North and Baltic Sea on local and regional atmospheric mercury transport.

2. Model description and set-up

2.1 Atmospheric modelling

Model description

To determine the mercury concentration in and the deposition from the atmosphere we used the chemistry transport model (CTM) CMAQ (Community Model for Air Quality). The CMAQ modelling system was developed by the U.S. EPA and is currently one of the most used CTMs worldwide (Byun & Ching, 1999; Byun & Schere, 2006). Here, we used CMAQ version 5.0.1 with the carbon bond chemistry mechanism version 5 including updated toluene chemistry and improved chlorine reactions: *cb05tump* (Tanaka et al., 2003; Sarwar et al., 2007), and the multi pollutant aerosol module aero6 (Yarwood et al., 2005; Whitten et. al., 2010). The mercury chemistry in CMAQ is based on the implementation of Bullock and Brehme (2002) but was updated based on observations and model inter-comparisons in the course of the EU FP7 project GMOS (Global Mercury Observation System) (Bieser et al., 2014) (Eq. 1-1 to 1-5). CMAQ includes three mercury species in the atmosphere: Gaseous Elemental Mercury (GEM), Gaseous Oxidized Mercury (GOM), and Particle Bound Mercury (PBM). To determine the exchange of mercury between the atmosphere and other environmental compartments we utilized a bi-directional flux implementation by Bash (2010). For the default CMAQ runs the dry deposition velocity of mercury is set to zero above water bodies and the net deposition is calculated using a fixed concentration for mercury in the surface ocean (Bash, 2010). In a second step we re-run CMAQ for the years 2000 and 2005 using the air-sea exchange calculated by the ocean-ecosystem-chemistry model instead for the North- and Baltic Sea, considering the following reactions:

$$GEM + O_3 \rightarrow GOM \quad (1\text{-}1)$$

$$GEM + OH \rightarrow GOM \quad (1\text{-}2)$$

$$GEM + H_2O_2 \rightarrow GOM \quad (1\text{-}3)$$

$$GEM + Cl_2 \rightarrow GOM \quad (1\text{-}4)$$

$$GEM + Cl + M \rightarrow GOM + M \quad (1\text{-}5)$$

where M is a non-reactive molecule (e.g. O_2, N_2).

Atmospheric emissions data and regional meteorology

Emission data for primary pollutants and precursors of ozone and secondary particulate matter were created with the SMOKE for Europe emission model (Bieser et al., 2011a) which is based on the US-EPA emission model SMOKE (Houyoux et al., 2000; UNC, 2005). Biogenic emissions and NO emissions from soils were created with the BEIS3.14 biogenic bottom-up emission model (Pierce et. al., 2002; Vukovich and Pierce, 2002; Schwede et al., 2005). Additionally, we used the AMAP emission inventories for the years 1990, 1995, 2000, 2005, and 2010 as source for gridded annual mercury emissions (Pacyna et al., 2003, 2006b, Wilson et al., 2010). The SMOKE-EU model was used to temporally disaggregate these emissions to create the hourly fields needed as CMAQ input (Bieser et al., 2011a). The speciation between the three mercury species was based on observations by Weigelt et al. (in prep.) and the vertical distribution was based on plume rise profiles by Bieser et al. (2011b). Finally, boundary conditions for the regional domain were taken from monthly means of the TM5 global CTM (Huijnen et al., 2010) provided by the Dutch Royal Meteorological Institute (KNMI). For the mercury species we used boundary fields from the global CTM GLEMOS (Travnikov and Ilyin, 2009).

All physical atmospheric parameters were taken from regional atmospheric simulations with the COSMO-CLM mesoscale meteorological model (version 4.8) for the years 1990, 1995, 2000, 2005, and 2010 (Geyer, 2014) using NCEP reanalysis data as forcing (Kalnay et al., 1996). COSMO-CLM is the climate version of the regional scale meteorological community model COSMO (Rockel et al., 2008), originally developed by Deutscher Wetterdienst (DWD) (Steppeler et al., 2003; Schaettler et al. 2008). It has been run on a 0.22° x 0.22° grid using 40 vertical layers up to 20 hPa for entire Europe. COSMO-CLM uses the TERRA-ML land surface model (Schrodin and Heise, 2001), a TKE closure scheme for the planetary boundary layer (Doms, 2011; Doms et al., 2011), cloud microphysics after Seifert and Beheng (2001, 2006), the Tiedtke scheme (Tiedtke, 1989) for cumulus clouds and a long wave radiation scheme following Ritter and Geleyn (1992). The meteorological fields were then processed to match the CMAQ grid. CMAQ uses the information that is provided by the meteorological input fields to calculate transport, transformation and loss of all gas phase and particulate species. The impact of the meteorological fields on the output of the chemistry transport model was investigated in detail in the articles by Matthias et al. (2009) and Bieser et al. (2011a).

Model setup

The atmospheric model domain covers the entire European land mass, including north Africa and western Russia with a resolution of 72x72km and 30 vertical layers (see Fig. 1a). CMAQ is initialized by a mean concentration field and a spin up time of 14 days is used. The model uses a resolution dependent internal time step of 450 seconds and creates hourly output fields. Due to computational limitations it was not possible to create a continuous simulation and CMAQ was instead only run for every fifth year (1990, 1995, 2000, 2005, 2010).

2.2 Ocean modelling

Model description

Calculations of mercury cycling in the ocean are based on the ocean-ecosystem model ECOSMO (Schrum et al., 2006; Daewel & Schrum, 2013). ECOSMO is a regional 3-d Eulerian model that considers hydrodynamics, sea ice and bio-geochemical cycling including phyto- and zooplankton production. The ocean hydrodynamics are simulated considering time dependent surface elevation and sea ice dynamics. The hydrodynamic model is a non-linear hydrostatic z-level model, which is using semi-implicit, energy and entropy conserving numerical methods. Scalar properties are advected using a shape-preserving total variation diminishing numerical

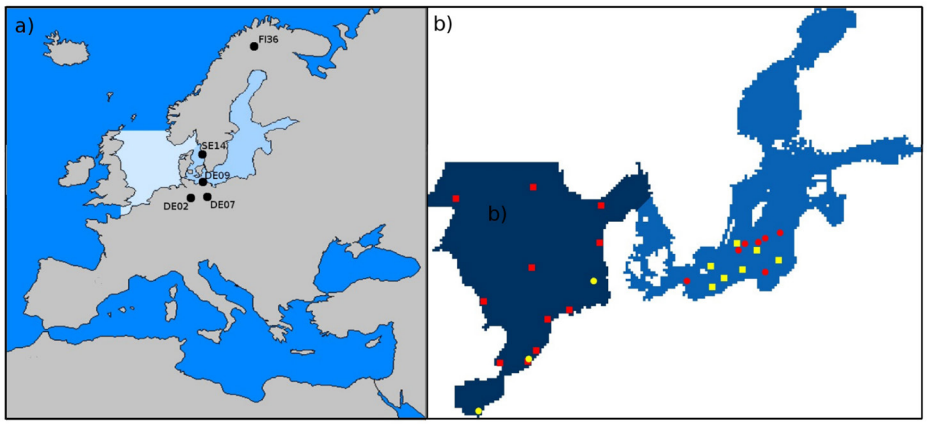

Figure 1

Model domain and sampling locations.

a) CMAQ model domain and location of EMEP measurement stations. b) MECOSMO domain and sampling locations from ship cruises. North Sea: red squares (Coquery and Cossa, 1992), yellow circles (Baeyens and Leermakers, 1998). Baltic Sea: yellow squares winter 1997, red circles summer 1998 (Wängberg et al., 2001).

doi: 10.12952/journal.elementa.000111.f001

scheme. The hydrodynamic model is in detail described in Schrum and Backhaus (1999) and recent numerical updates were described by Barthel et al. (2012). The ocean bio-geochemical cycling and plankton production is resolved through simulation of 3 limiting macro-nutrient cycles, the nitrogen-, the silicon and the phosphorus cycle and oxygen. The model resolves three plankton groups, diatoms, flagellates and cyanobacteria, and two zooplankton groups. The organic matter cycling is furthermore resolved by dissolved and particulate matter groups and a simple organic surface sediment pool. A detailed model description of the bio-geochemical cycling is given by Daewel and Schrum (2013).

To implement mercury chemistry in the ECOSMO framework we introduced the species elemental mercury, inorganic oxidized mercury, and methylated mercury into the model. While elemental mercury is always treated as dissolved (DEM) in the aqueous phase, oxidized mercury (Hg^{II}) is either dissolved or associated to particles (PBM). Moreover, for particulate bound mercury we distinguish between three kinds of particles: phytoplankton (BPC), zooplankton (BZC), and inanimate particulate organic carbon (POC). Here we assume that only mercury bound to POC has a sinking velocity (3.5 m/day) and can accumulate in the sediment. For the dissolved-particle partitioning we use a partitioning approach following Brigham et al. (2009), assuming an instantaneous equilibrium at each time step. The partitioning coefficient K_d varies between $3x10^4$ and $7x10^5$ [l/kg] depending on the amount of dissolved organic matter (DOM), which is estimated based on dissolved organic carbon (DOC) in the aqueous phase following Eq. 2-1 and 2-2:

$$K_d = 0.22865 * \exp(0.7505 * DOM) \quad (2\text{-}1)$$

$$PBM = K_d * POM * Hg^{II} * 10^6 \quad (2\text{-}2)$$

where DOM is dissolved organic matter in [mg/l]; POM is particulate organic matter in [mg/l]; K_d is the partition coefficient in [l/kg]; PBM is Hg^{II} bound to particles in [ng/l]; and Hg^{II} is the sum of dissolved Hg^{II} and PBM in [ng/l].

Depending on the salinity, which varies between 1 PSU and 35 PSU in our model domain, up to 40% of the dissolved Hg^{II} is considered to be bound in chlorine complexes and is not available for reduction (Mason et al., 1996). Thus, compared to the North Sea, there is a higher reduction potential of Hg^{II} in the Baltic Sea and near large estuaries where the salinity is much lower than 35 PSU.

Inorganic chemical reactions considered are dark- and photo-oxidation of DEM as well as photolysis and biologically induced reduction of the dissolved Hg^{II} not bound as chlorine complexes (Table 1). Reaction rates for inorganic mercury species are based on Soerensen et al. (2010) and Qureshi et al. (2010). In the model, all reactions are implemented as pseudo-1st order reactions following Eq. 3-1:

$$C_t = C_0 * \exp(-a*k*t) \quad (3\text{-}1)$$

where k is the reaction rate [see Table 1 for units]; a is a constant depending on the reaction rate (e.g. Dissolved organic matter in [mg/l]); t is time in [s]; C_t is concentration at time t in [ng/l]; and C_o is initial concentration in [ng/l].

Moreover, it is important to consider methylation processes in the ocean, because MeHg can be an important sink for Hg^{II}. Especially during the warm seasons, a significant fraction of the total aqueous mercury can be in organic form and thus the amount of DEM is indirectly influenced by the amount of methylated mercury. Currently, we consider only bulk methylation and de-methylation of mercury in the model. The exact mechanics of mercury methylation are still unclear and published reaction rates show a very high variability (Sonke et al., 2013). For example, Monperrus et al. (2007) and Lehnherr et al. (2011) measured methylations rates in the range of $4.4x10^{-7}$ to $2.3x10^{-9}$ s^{-1} and de-methylation rates in the range of $4.9x10^{-6}$ and $5.7x10^{-9}$ s^{-1}. For this study we used estimated average values for total methylation, dark de-methylation, and photo induced de-methylation rates based on observations (Heyes et al., 2006, Monperrus et al., 2007, Ranchou-Peyruse et al., 2009) (Table 1).

All non-photolytic reactions can also take place in the sediment. A simple 2-layer sediment compartment was implemented following the approach chosen for the ECOSMO bio-geochemical model with the upper layer exchanging dissolved mercury from pore water with the water column above. In cases of high friction velocities (>0.01 m/s) the particulate mercury in the first sediment layer can be re-suspended. The second sediment layer represents a permanent sink for mercury based on a fixed burial rate from the top sediment layer of (0.00001 d^{-1}).

Finally, the potential air-sea exchange of elemental mercury is calculated using the temperature dependent Henry constant (Eq. 4-1) for mercury from Andersson et al. (2008). The velocity of the exchange between the two compartments is dominated by the mass transfer coefficient in the aqueous phase. We calculated this coefficient using a parametrization for wind speed dependency from Nightingale et al. (2000) and included a temperature correction for the diffusivity of mercury according to Kuss (2014) (Eq. 4-2). A detailed description

Table 1. Reaction rates for aquatic mercury reactions

Reaction	Rate	Unit
Dark oxidation	1.0E-7	s^{-1}
Photo oxidation	6.6E-6	$ng^2\ W^{-1}\ s^{-1}$
Photo reduction	1.7E-6	$ng^2\ W^{-1}\ s^{-1}$
Bio reduction	4.5E-6	$l\ mg^{-1}\ s^{-1}$
Methylation	1.0E-8	s^{-1}
Dark demethylation	1.0E-8	s^{-1}
Photo demethylation	1.0E-9	$ng^2\ W^{-1}\ s^{-1}$

doi: 10.12952/journal.elementa.000111.t001

of the method can be found in Qureshi (2011). Sea ice is seasonally important in the Baltic Sea, in severe winters it might extend over almost the entire area. In case of sea ice presence, the air-sea exchange is limited to the open water fraction of a grid cell (Eq. 4-3). Mercury exchange between atmosphere and sea ice as well as ocean and sea ice is currently neglected. The relevant equations are:

$$H = \exp[-2404.3 / (T + 6.915)] \quad (4\text{-}1)$$

$$kw = (0.0025 * U10^2) * (0.0315 * (T - 273.15) + 0.784) \quad (4\text{-}2)$$

$$F_{wa} = (1 - F_{ice}) * kw * (C_{aq} - C_{air} / H) \quad (4\text{-}3)$$

where T is temperature in [K]; H is the Henry constant for mercury which is dimensionless; kw is the mass transfer coefficient in [m/h]; U10 is the wind speed at 10m in [m/s]; C_{aq} is the mercury concentration in water in [pg/l]; C_{air} is the mercury concentration in air in [ng/m^3]; F_{ice} is the fraction of ice coverage which is dimensionless; and F_{wa} is the flux water to air in [ng/m^2 h].

Mercury riverine loads and emission data

Mercury sources to the ocean-sediment system are mainly from riverine loads and from atmospheric deposition. Atmospheric mercury wet and dry deposition was taken from CMAQ. The dry deposition of GEM was turned off over water bodies. The river loads were implemented as annual and, where possible, as monthly average values based on national reported water borne loads to the North Sea, as reported by OSPAR (Oslo and Paris Commission, Protecting and conserving the North-East Atlantic and its resources) and retrieved for the Norwegian National Pollution Assessment for the North Sea waters (Green et al., 2011) (see Section 4.2). For the Baltic Sea we used annual fluxes as reported by HELCOM (Helsinki Commission, Baltic Sea Marine Environment Protection Commission), (HELCOM, 2011). Missing data was filled based on the HELCOM (2007) report leading to a riverine mercury inflow of 1100 kg/a into the Baltic Sea. Finally, initial sediment concentrations for the deep basins in the North Sea (Kersten et al., 1988; Leermakers et al., 2001) and Baltic Sea (Borg and Jonsson, 1995; Pempkowiak et al., 1998; Beldowski and Pempkowiak, 2003) were implemented based on observations.

Model setup

The ocean model ECOSMO was setup on a model domain covering the entire Baltic Sea and the North Sea (Fig. 1b). Open boundaries are in the English Channel and at 63° North, where the North Sea is connected to the Atlantic. The resolution of the model is about 10x10 km^2 (spherical grid) with a top layer depth of 5m and up to 20 layers to resolve the vertical direction up to a maximum water depth of 630m. The ocean mercury model was run for the time span 1993 to 2008. Hydrodynamics and ocean bio-geochemistry data were taken from an earlier published and in detail validated multi-decadal ocean model hindcast (Daewel & Schrum, 2013). Ocean mercury concentrations are transported in the water column using daily mean currents, sea level and turbulence from the existing long-term simulation. The Eulerian advection-turbulent diffusion algorithm used for the mercury transport in the ocean is the same as in the ECOSMO model (Daewel & Schrum, 2013; Barthel et al., 2012). Partitioning and chemical speciation of mercury in the ocean are calculated using the daily mean temperature, salinity, plankton-, organic matter- and sediment carbon contents from the long-term simulation. Light conditions used to calculate photolytic reactions are calculated in a similar way as in the ECOSMO model (Daewel & Schrum, 2013). The internal time step of the chemical ocean module is 600 seconds and the output fields are daily average values.

We created an initial concentration field for all mercury species to start the model in a quasi realistic state. For this, we interpolated 1452 observations of mercury in the North and Baltic Sea between 1980 and 2010 using a bi-linear interpolation approach. The observational mercury data were retrieved from the ICES

(The International Council for the Exploration of the Sea) database (http://ecosystemdata.ices.dk/, http://www.ices.dk/marine-data/data-portals/Pages/ocean.aspx) and manually corrected for outliers. At the boundaries to the Atlantic ocean, we mirrored Hg concentrations from the outer most MECOSMO model grid cells. As spin up we let the uncoupled model run 15 years using GEM concentration and deposition fields from CMAQ. For this, we used the CMAQ runs described above, which were performed for every fifth year and used interpolated data for the years in between.

Finally, to determine the air-sea exchange and its impact on the regional transport patterns of mercury in Europe, we run MECOSMO-CMAQ coupled for two selected years 2000 and 2005. We chose these years after evaluating the availability of observations on elemental mercury in the surface ocean, air-sea exchange, and atmospheric mercury concentrations. For the coupled run we let the models run stand alone and exchange data using the output time step of one day.

3. Model evaluation

For the evaluation of the modelled air-sea exchange we used measurements of GEM in the atmosphere and DGM in the surface ocean. Because dimethylmercury is currently not implemented into the model we compare measured DGM concentrations to modelled DEM concentrations. The negligence of dimethlymercury in the model could lead to an underestimation of DGM concentrations. However, according to unpublished measurements of Kuss et al. (personal communication) dimethylmercury makes up only about 1% of the DGM measured in the Baltic Sea.

In the atmosphere we use data from five EMEP stations. This includes a remote station FI36 (Pallas, Finland), two coastal stations DE09 (Zingst, Germany) and SE14 (Raö, Sweden), and two downwind stations DE02 (Waldhof, Germany) and DE07 (Neuglobsow, Germany) to evaluate the impact of the air-sea exchange on the regional transport of mercury (Fig. 1a).

In addition, shipborne observations from seven cruises in the western and central Baltic Sea are used for the model evaluation. This includes two cruises in the central Baltic Sea in 1997 and 1998 where both marine and atmospheric mercury concentrations were measured (Wängberg et al., 2001), one cruise in 2000 where total mercury concentrations near the German coast were observed (Wurl et al., 2001), and four cruises in 2006 to evaluate the seasonal variability of the air-sea exchange (Kuss and Schneider, 2007). Moreover, observations at Swedish rivers and coastline from Garfeldt et al., (2001) are used to evaluate the impact of river inflow. Finally, we use DEM observations from three cruises in the North Sea (Coquery and Cossa, 1992, 1995) and data from a platform in the German Bight (Baeyens and Leermakers, 1998). The sample locations are given in Fig. 1b for those cruises where they were reported. For some cruises only approximate sampling locations could be obtained.

3.1 Dissolved elemental mercury

Only a small fraction of mercury in the ocean exists as elemental Hg^0. In order to model the air-sea exchange of mercury the model needs to be capable of reproducing dissolved elemental mercury (DEM) concentrations in the surface water. Zhijia et al. (2011) published a global review on DGM concentrations at coastal sites. They report DGM concentrations at coastal sites between 6 pg/l and 176 pg/l, and for the Baltic Sea between 17 and 100 pg/l. These values are comparable to the modelled DEM concentrations in the range of 10–80 pg/l. In river inflow grid cells the model calculates DEM concentrations in the range of 200 pg/l up to 1000 pg/l. This is in line with the findings of Garfeldt et al. (2001) who report more than 10 times higher concentrations in rivers at the Swedish coast compared to seawater. Moreover, Wurl et al. (2001) measured total mercury concentrations in the range of 200 to 1870 pg/l in the Belt Sea during winter 2000.

For the model evaluation we compared 413 DGM measurements in the Baltic Sea between 1997 and 2006 to modelled DEM concentrations. 83% of the model values were found to be within a factor of 2 of the observations and 16% of the model values are within the uncertainty of the observations of 10%. It was found that, on average, the model (11.3±4.1 pg/l) tends to underestimate observed DGM concentrations (15.4±5.1 pg/l) by 25% but is able to reproduce the observed variability (Table 2). The model performance is similar throughout the year (NME: Feb = 0.28, Apr = 0.41, Jul = 0.31, Nov = 0.30). The seasonal differences can be explained by different sampling locations rather than different model behaviour. These results seem remarkable, given that atmospheric models typically reproduce TGM concentrations within an accuracy of 10% (Bullock et al., 2008).

Fig. 2 depicts all DGM measurements in the Baltic Sea used for model evaluation separated by season and region of sampling. Samples taken in the same model grid cell on the same day were averaged. It can be seen, that the model performs best in the Belt and Arkona Sea throughout the year. Moreover, for this region the model performs similarly for different years as can be seen by comparison to observations from 1997, 1998, and 2006. In the Bornholm Sea, the model underestimates the variability during April and November but not during February and July. The variability of Hg concentrations in this region is mainly

Table 2. Comparison of modelled ocean surface DEM concentrations with observations from six cruises in the Baltic Sea for different seasons (Wängberg et al., 2001, Kuss and Schneider, 2007)[a]

Time of sampling	NMB[b]	MNB[c]	MNE[d]	N
February and March	-0.25	-0.26	0.28	81
April	-0.41	-0.41	0.41	81
July	-0.32	-0.29	0.31	95
November	-0.06	-0.03	0.30	156
Annual	-0.27	-0.23	0.32	413

[a]The formulas for the statistics are given in Appendix A.
[b]NMB=Normalized Mean Bias.
[c]MNB=Mean Normalized Bias.
[d]MNE=Mean Normalized Error.
doi: 10.12952/journal.elementa.000111.t002

driven by the transport of riverine inflow from the German and Polish coast. Thus, the missing variability in April and November could be due to the modelled transport patterns at the time of the cruise or the missing inter-annual variability of the riverine inflow in this region. Finally, in the Gotland Sea both, model (5–30 pg/l) and observations (10–35 pg/l) indicate a high variability of DEM concentrations (Fig. 3). In this region, the model evaluation is strongly dependent on the sampling location and time as the modelled DEM concentrations can vary by 5 pg/l and more between days and neighbouring grid cells. Here, the model predicts a strong gradient between the southern and northern Gotland Sea. Unfortunately, there are no measurements further north to validate this modelled gradient.

The DEM concentrations depend (among others) on temperature, solar radiation, biological activity, and atmospheric GEM concentration (Kuss et al., 2015). In order to evaluate the capability of the model to reproduce the seasonal variability we compared modelled normalized seasonal concentrations to observations from a series of ship cruises from 2006 (Kuss and Schneider, 2007). The observations indicate increased DGM concentrations during spring and summer with the peaks becoming more pronounced from west to east (from west to east: Belt, Arkona, Bornholm, Gotland Sea, Bothnian Sea). For all regions, the model is able to reproduce this general seasonal cycle. In the Arkona Sea the model overestimates the summer peak by 20% and underestimates the winter minimum by 20%. In the Bornholm Sea, the model leads to higher values during winter than the observations. For the Bothnian Sea, where no observations are available, the model gives a similar seasonal cycle as for the Gotland Sea but with an even more pronounced summer peak.

For the North Sea, there are less DGM observations available compared to the Baltic Sea (Fig. 1b). All available observations date back to the 1990ties a time when the measurement uncertainty was higher (up to 50%) compared to today's methods. Moreover, there is no information on the fraction of dimethylmercury. In May 1996, Baeyens and Leermakers (1998) observed DGM concentrations of 12.0 pg/l at a platform in the German Bight. In the corresponding grid cell modelled average concentrations for May are 10.2 pg/l. For the Schelde Estuarie, they report DGM concentrations of 42-50 pg/l for winter and 80-108 pg/l for summer. The model gives 35–78 pg/l for winter and 93–247 pg/l for summer 1996. Coquery and Cossa (1992, 1995) published DGM concentrations for 18 samples taken all over the North Sea in July 1991. Unfortunately, the MECOSMO runs do not include this year. However, these observations were compared to model data from 1996. For July 1991 Coquery and Cossa (1995) found DEM concentrations at the Schelde estuary in the range of 36–90 pg/l. This is comparable to findings from Baeyens and Leermakers (1998) for the year 1996. Also at other estuaries the model compares well with observations (Fig. 4). At the Danish North Sea coast (orbs: 38 pg/l) and in the Skaggerag (obs: 84 pg/l) the model exhibits strong local DEM peaks whose location differs from year to year. Here, the model gives DEM concentrations up to 50 pg/l (also see Fig. 9 in Section 4.2). Also in the northern, open North Sea high DGM concentrations were observed: Scottish coast (obs: 42 pg/l) and Norwegian coast (obs: 70 pg/l). In the model, DEM concentrations in this region vary between 10–40 pg/l during summer and 20–80 pg/l in spring. Finally, Coquery and Cossa (1995) report DEM concentrations in the central Baltic to be lower than the detection limit of their method (20 pg/l). For this region the model gives DEM concentrations between 5 and 10 pg/l. This is also in line with the observations by Baeyens and Leermakers (1998) with 12 pg/l in the German Bight.

3.2 Air-sea exchange

The evaluation of air-sea fluxes calculated with MECOSMO-CMAQ is difficult because there are no direct measurements available. Observation based fluxes are calculated using measurements of DGM and TGM (Wängberg et al., 2001; Kuss and Schneider; 2007). Based on the observed wind speed and water temperature, different parametrizations for the Henry's Law constant, the diffusivity of gaseous mercury in

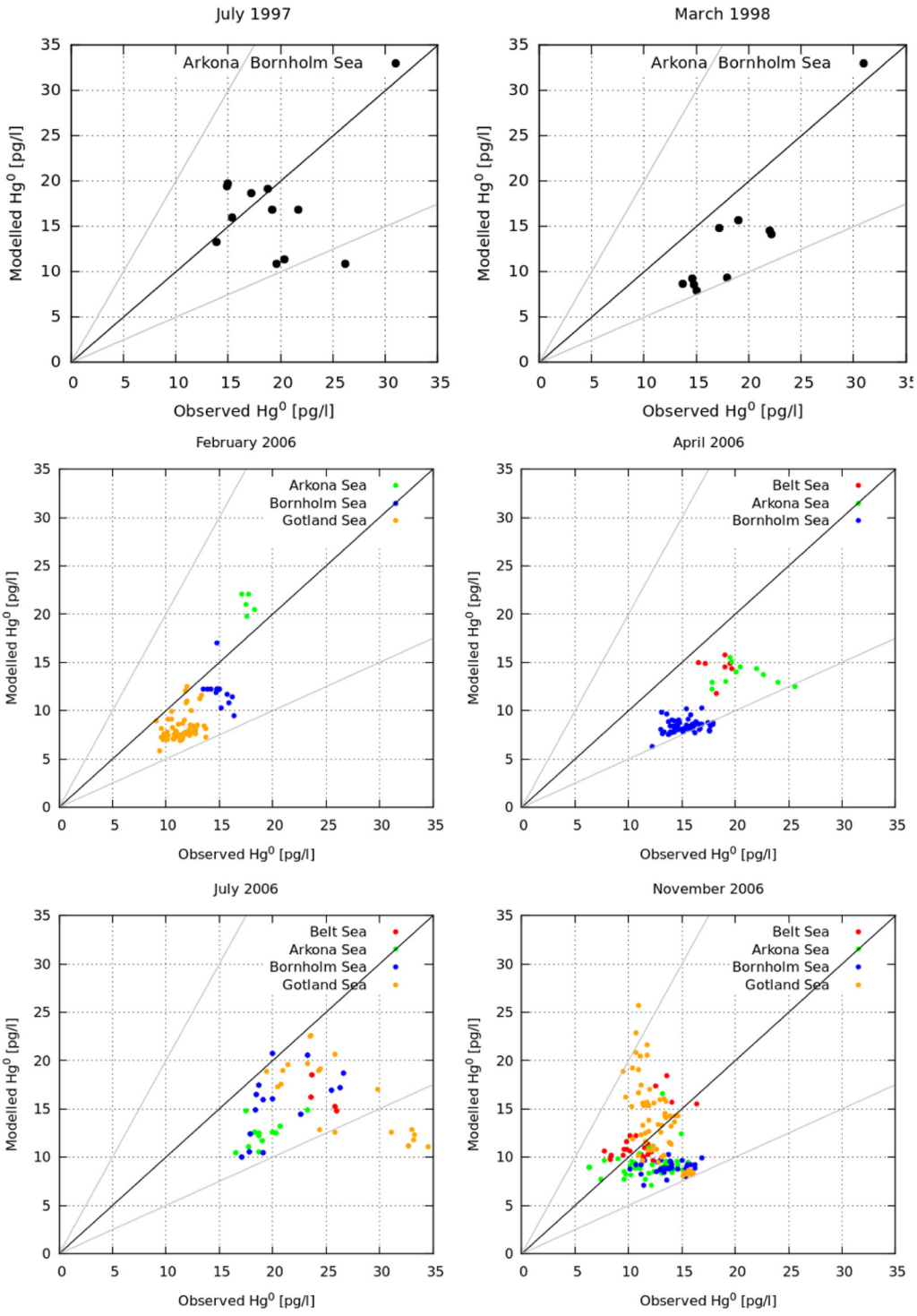

Figure 2

Comparison of observed and modelled Hg^0 concentrations in the Baltic Sea.

Comparison of observed and modelled DEM concentrations in different parts of the Baltic Sea. Data is based on Wängberg et al. (2001) and Schneider and Kuss (2007). The sampling locations for the data from Wängberg et al. (2001) are depicted in Fig. 2. Values between the grey lines are within a factor of 2. Observations are DGM and model values Hg^0 concentrations.

doi: 10.12952/journal.elementa.000111.f002

water, and the transfer velocity between the compartments are used to calculate an effective Hg flux (see Section 2.2). Wängberg et al. (2001) calculated fluxes using a parametrization based on Wanninkhof (1992) and Kuss and Schneider (2007) a parametrization based on Weiss et al. (2007). Both exhibit a stronger wind dependency than the parametrization used in this study (Nightingale et al., 2000; Kuss, 2014). Based on DGM and TGM data published by Wängberg et al. (2001) and Kuss and Schneider (2007) we recalculated the observed air-sea fluxes according to equations 4-1 to 4-3. We found, that the differences between the various flux parameterizations were in the same order of magnitude as the differences between modelled and observed fluxes when using the same parametrization which is in line with the findings of Strode et al.

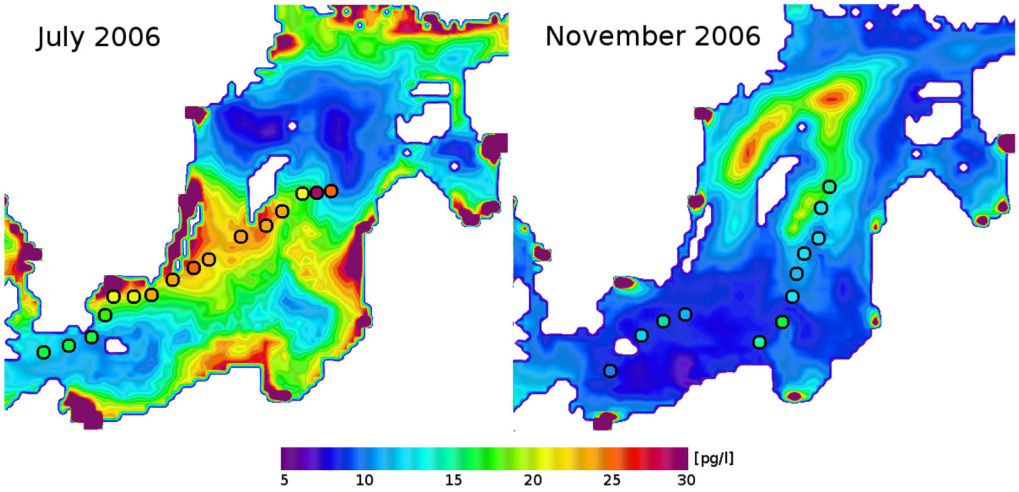

Figure 3

Modelled and observed spatial variability of Hg^0 in the central Baltic Sea.

Modelled daily average DEM concentrations for 7.7.2016 (left) and 12.11.2016 (right) plotted against DGM observations from 6-8.7 and 11-13.11 (Kuss and Schneider, 2007).

doi: 10.12952/journal.elementa.000111.f003

(2007). This makes it difficult to assess the real mercury flux between atmosphere and ocean. However, we think that the Hg flux is a good metric to assess the performance of a coupled modelling system as it includes concentrations both in the atmosphere and in the ocean.

Fig. 5 depicts modelled daily average air-sea fluxes for different regions of the Baltic Sea. In addition, the 60% and 90% quantile ranges are given to indicate the regional variability. The largest variability was found in the East Gotland Sea and the Bothnian Sea. This is due to the strong modelled DEM gradients in these regions (Fig. 3). Generally, all regions exhibit a similar behaviour with near zero fluxes in winter where the Baltic Sea can even become a sink for atmospheric mercury in the Bornholm Sea, Gotland Sea, and Bothnian Sea. These model results are in line with observations from Kuss and Schneider (2007) which show a near zero or even positive mercury air-sea flux (Fig. 5). During April, observations indicate a slightly higher Hg evasion than the model. However, the differences are small and well inside the range of uncertainty of air-sea flux parametrizations. During July, the model underestimates the evasion in the Belt Sea and the Arkona Sea. In the Gotland Sea, during July, the modelled peak fluxes are in the same range as the observations. However, the modelled mean fluxes are lower than the observations. Finally, during November, the modelled average fluxes are in good agreement with observations.

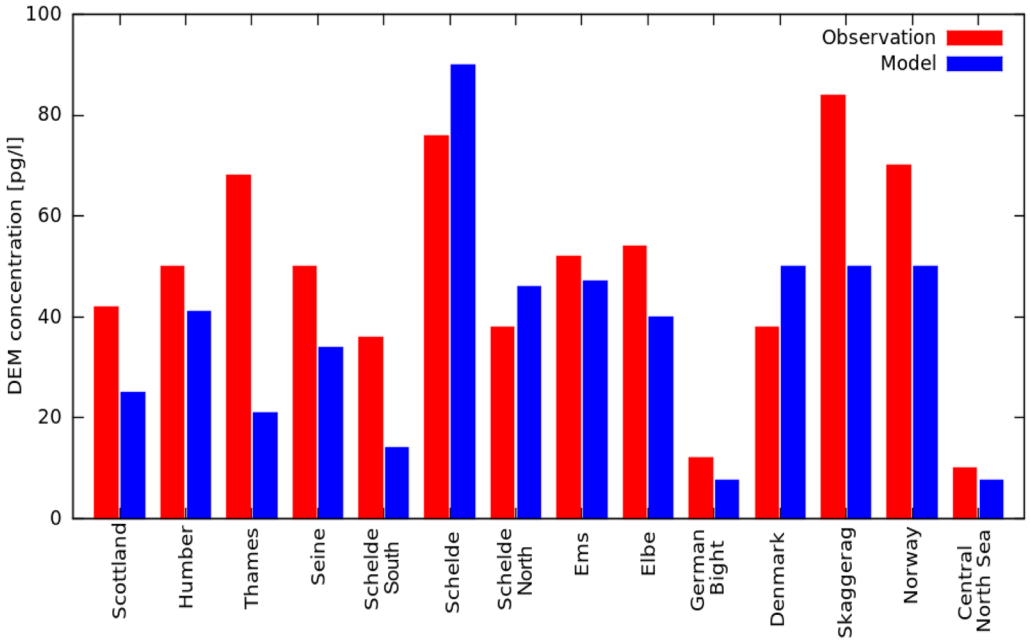

Figure 4

Comparison of observed and modelled Hg^0 concentrations in the North Sea.

Comparison of observed and modelled dissolved elemental mercury concentration in the North Sea with DGM observations (Coquery and Cossa, 1995; Baeyens and Leermakers, 1998). The sampling locations are depicted in Fig. 2.

doi: 10.12952/journal.elementa.000111.f004

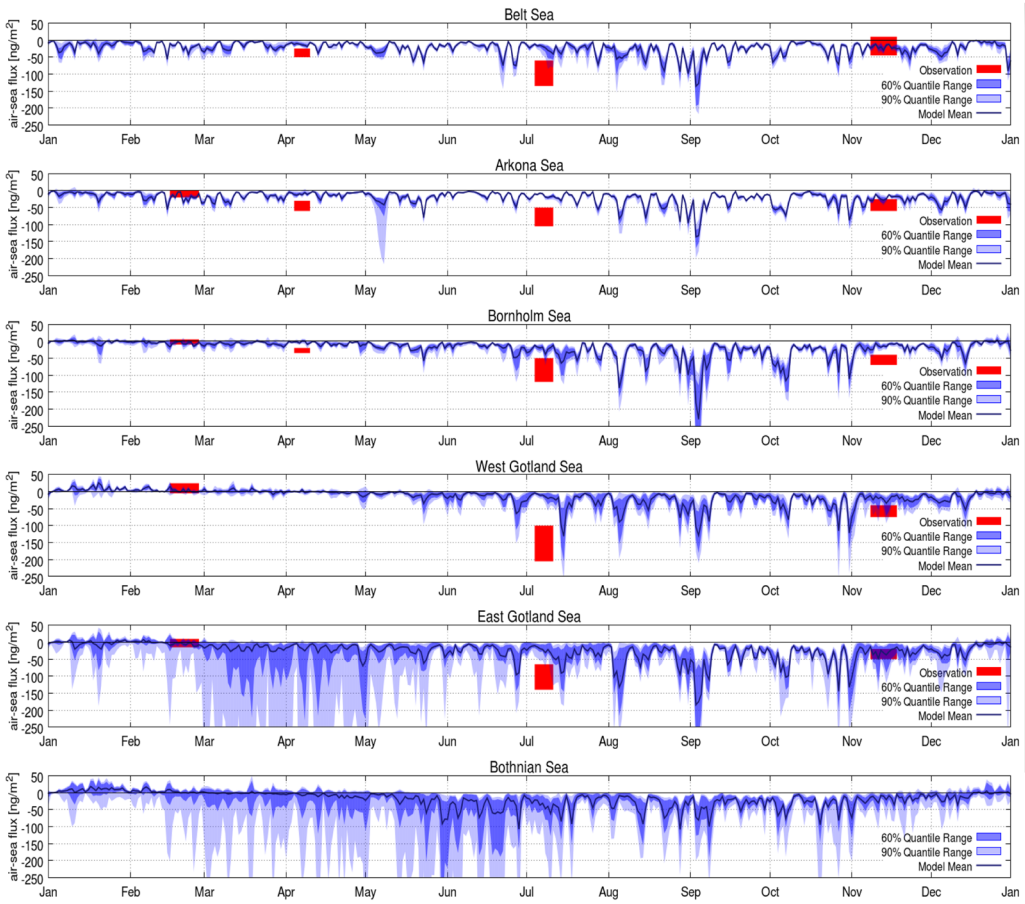

Figure 5

Seasonal variability of air-sea flux for different regions of the Baltic Sea.

Observations (red boxes) are based on data by Kuss and Schneider (2007). Model values are the regional average (blue line), the 60% quantile range (blue area), and the 90% quantile range (light-blue area). Negative values indicate a flux out of the ocean into the atmosphere.

doi: 10.12952/journal.elementa.000111.f005

3.3 Atmospheric mercury concentrations

In Table 3 the normalized mean bias (NMB) of modelled gaseous elemental mercury (GEM) is given for the years 2000 and 2005 for the five EMEP stations (see Fig. 1a) as calculated by CMAQ and ECOSMO-CMAQ. It can be seen, that the CMAQ run tends to underestimate GEM concentrations. On average, the model bias is around -10%. This value is dominated by a strong underestimation of GEM at Waldhof (-0.29). The evaluation is based on daily observations with a sample size of: Zingst N=365, Raö N=83, Pallas N=365, Neuglobsow N=8784, Waldhof N=39528.

The best agreement between model and observation is found for FI36 which is not deemed to be influenced by air-sea exchange due to its inland location north of the Baltic Sea. For Raö, model and observations are also in good agreement for 1995 (NMB=-0.02) and 2000 (NMB=0.02). However, in 2005 the model underestimates the GEM concentrations by 16% at Raö. This is due to an episode with polluted air masses not captured by CMAQ. At Zingst, the model constantly underestimates GEM concentrations by about 10%.

When running CMAQ using the air-sea fluxes calculated by MECOSMO and comparing to the default CMAQ simulation we see no change in concentrations at Pallas and only a small increase of GEM concentrations of 2% at Raö. However, in Zingst GEM concentrations increase by 5 to 10% and the coupled

Table 3. Normalized Mean Bias for EMEP stations in the Baltic Sea region with (right) and without (left) air-sea exchange of mercury

Station	2000		2005	
	CMAQ	CMAQ-MECOSMO	CMAQ	CMAQ-MECOSMO
DE09, Zingst	-0.11	0.00	-0.10	-0.04
SE14, Raö	0.02	0.03	-0.16	-0.14
FI36, Pallas	-0.06	-0.06	-0.03	-0.02
DE02 Waldhof	-	-	-0.29	-0.26
DE07 Neuglobsow	-	-	-0.13	-0.12

doi: 10.12952/journal.elementa.000111.t003

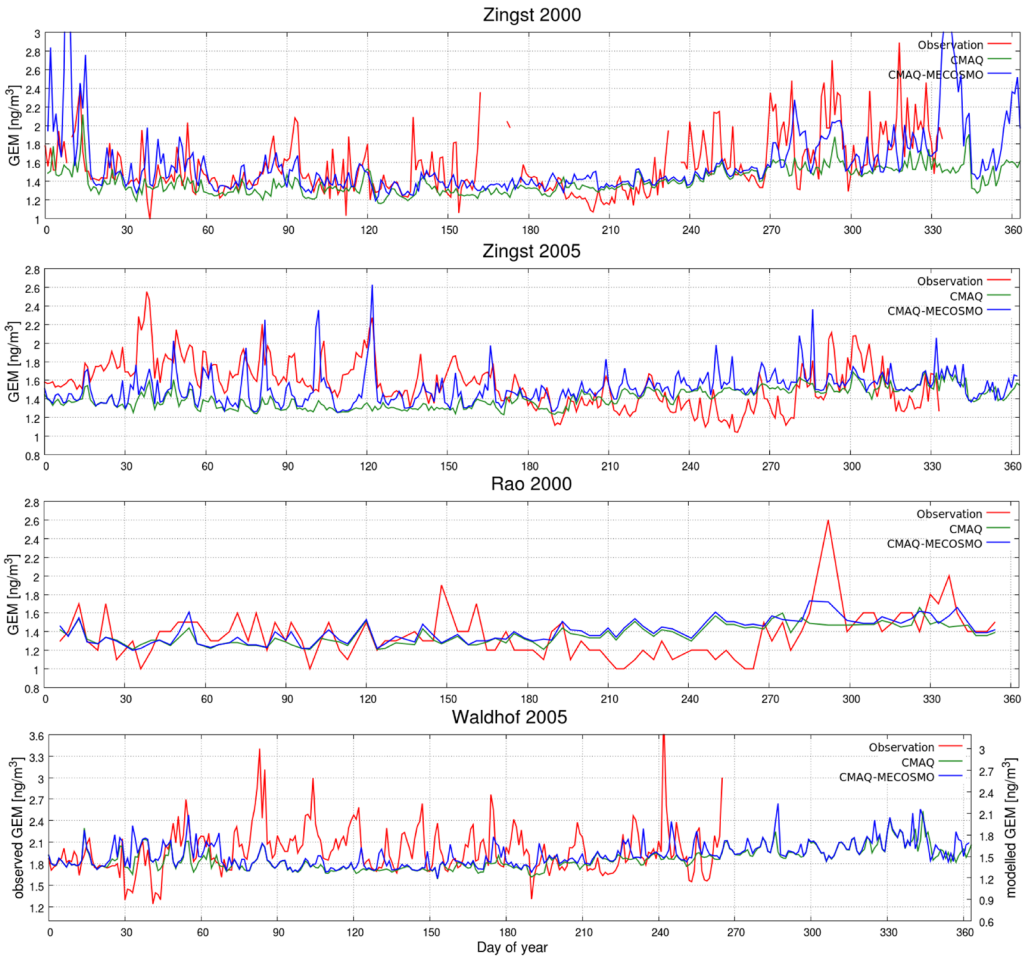

Figure 6

Comparison of observed and modelled atmospheric GEM concentrations.

Gaseous elemental mercury concentration at DE09 Zingst for the year 2000 (top) and 2005 (bottom) with (blue line) and without (green line) coupling to the ocean model. Statistics for this and other stations are given in Table 3.

doi: 10.12952/journal.elementa.000111.f006

model is in very good agreement with observations (Table 3). Moreover, the model is now able to reproduce several peaks observed at Zinst (Fig. 6). At Raö only a small number of GEM peaks is observed, which might be rather due to the low resolution of the observations as because of their absence. At Waldhof (+4%) and Neuglobsow (+2%), the air-sea exchange has a smaller, albeit positive, effect on modelled GEM concentrations. Also at these stations the implementation of emissions from the Baltic Sea leads to a better reproduction of some peaks during summer and autumn observed at these stations. A comparison of CMAQ-MECOSMO results for 2000 and 2005 show similar effects on atmospheric GEM concentrations in both years on average decreasing the model bias by 33%.

4. Results and discussion

4.1 Air-sea exchange in the Baltic Sea

Fig. 7 depicts seasonally averaged DEM concentrations in the model surface layer. On average, the highest concentrations occur in summer and autumn with the largest DEM peaks found during spring. These peaks are directly linked to biological activity leading to increased reduction of oxidized mercury. The lowest DEM concentrations in the Belt, Arkona, and Bornholm Sea are found in winter. For the northern Gotland Sea and the Bothnian Sea lowest DEM concentrations occur during spring. This is due to the low biological activity during winter (and early spring in the northern part of the Baltic Sea) and due to winter mixing, which increases the surface mixed layer depth from roughly 10m to 20m in summer to around 100m in winter (e.g. Janssen et al., 1999). In shallow waters the amount of particulate matter is higher in winter compared to offshore waters because of near coastal resuspension induced by high wind speeds in winter. This leads to a larger fraction of mercury bound to particles, which is not available for reduction.

The highest DEM concentrations throughout the year are found near estuaries, especially, in the Gulf of Finland, the Bothnian Sea, and the Bay of Bothnia. These DEM peaks are due to the riverine inflow of mercury in these areas. Increased total mercury concentrations lead to increased DEM concentrations. Recently, Schartup et al. (2015) suggested that Hg bound to terrestrial DOM has a lower reactivity than Hg bound to marine DOM which means that the amount of reducible Hg^{II} in these areas could be overestimated in the model.

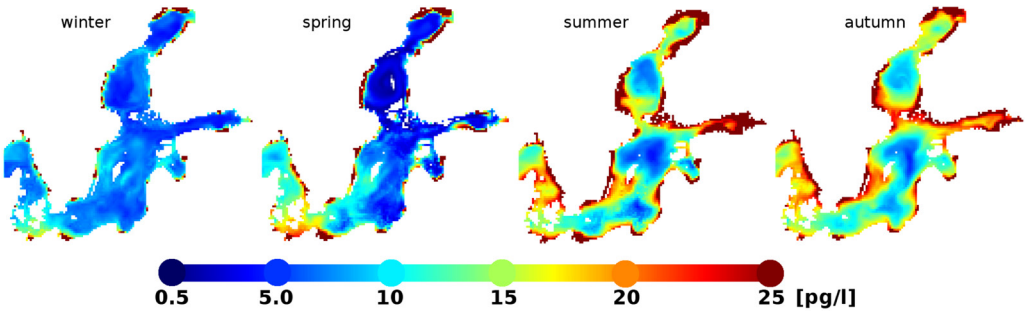

Figure 7

Modelled surface Hg^0 concentrations in the Baltic Sea.

Seasonally averaged dissolved elemental mercury (DEM) concentration in model surface layer (5m depth) for 1998. From left to right: winter (Dec-Feb), spring (Mar-May), summer (Jun-Aug), autumn (Sep-Nov).

doi: 10.12952/journal.elementa.000111.f007

The model indicates that there is an annual minimum in the north-eastern Gotland Basin and the Bothnian Sea. Here, average DEM concentrations as low as 2 pg/l are calculated by the model. In the Bothnian Bay the fraction of DEM compared to the total mercury concentration is higher than in the rest of the Baltic Sea, because of the higher reduction potential caused by the very low salinity (0-2 PSU at the northern most part of the Baltic Sea).

The variability of the air-sea exchange (Fig. 5 and 8) is mainly determined by the variability of DEM surface concentrations. GEM concentrations in the atmosphere vary between 1.2 and 2.0 ng/m^3. This equals a variability of 50% around the atmospheric average of 1.5 ng/m^3. In comparison, DEM shows a much larger variability on the seasonal scale (Fig. 7). However, the higher GEM concentrations in winter, which are caused by higher emissions and a lower planetary boundary layer, intensify the seasonal cycle of the air-sea exchange dominated by DEM. At typical winter temperatures DEM concentrations above 8 pg/l are needed for a Hg flux into the atmosphere. Because of the dependency on the Henry's Law constant and the diffusivity of gaseous mercury in the water, during summer only around 6 pg/l are needed for an effective Hg flux into the atmosphere. These values are estimated based on average values for atmospheric GEM concentrations, temperature, and the Henry's Law constant (Eq. 4-1) for winter and summer.

Table 4 gives seasonal DEM fluxes averaged over a 14 year period from 1994 to 2007. In the model, the central Baltic can become a sink for mercury during spring and in the northern part of the Gotland Sea and in the Bothnian Sea also during winter. The fluxes into the atmosphere are larger in the coastal regions following the DEM concentration gradients depicted in Fig. 7. We calculated the total mercury flux from the Baltic Sea, ignoring 10 river inflow grid cells which have very high DEM concentrations in the model. Observations at the Swedish coast by Garfeldt et al. (2001) indicate that DEM concentrations in rivers are more than 10 times higher than in the open ocean. In the model, river inflow grid cells have up to 10-20 times (100 – 300 pg/l) higher concentrations compared to the open ocean grid cells (5 – 30 pg/l).

The calculated average annual mercury evasion from the entire Baltic Sea is 3700±200 kg/a (winter 500±70 kg/a, spring 400±120 kg/a, summer 1300±80 kg/a, autumn 1500±100 kg/a). The inter-annual variability is 15% (3450 kg/a to 4000 kg/a). The air-sea exchange is dominated by the Gotland Sea (27%), the Bay of Bothnia (22%), and the Bothnian Sea (14%) which is responsible for 63% of the total mercury evasion in the Baltic Sea (Table 5). The North and East Gotland Sea as well as the Bothnian Sea are the only regions with a seasonal net influx into the ocean which occurs during spring time. The modelled average mercury flux for different regions of the Baltic Sea is given in Table 5. Kuss and Schneider (2007) estimated the annual mercury evasion from the central Baltic (235000 km^2) for 2006 to be in the range of 2700 kg/a – 5900 kg/a. For this region, which excludes the Gulfs of Bothnia, Finland, and Riga the model calculates a flux of 2100 kg/a for 2006. In order to calculate the net Hg budget we also take into account wet deposition (3300 - 3500 kg/a) modelled with CMAQ and the annual riverine Hg inflow of 1100 kg/a (HELCOM, 2007, 2011). This leads to an accumulation of Hg in the Baltic Sea in the range of 500-1000 kg/a. However, for a reliable estimation of the Baltic Hg budget more information on the riverine inflow is needed. The previous HELCOM report (2007) estimated the total riverine Hg inflow to be 6400 kg/a. A model run based on these river loads doubled the annual Hg evasion from the Baltic Sea (7450±500 kg/a).

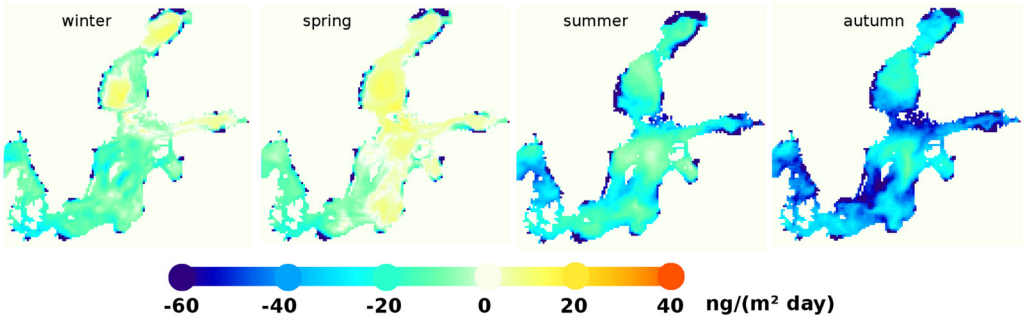

Figure 8

Modelled air-sea exchange of Hg^0 in the Baltic Sea.

Seasonally averaged daily air-sea flux for the Baltic Sea in 1998 (negative values indicate a flux into the atmosphere). From left to right: winter, spring, summer, autumn.

doi: 10.12952/journal.elementa.000111.f008

Table 4. Annual total mercury fluxes for the entire Baltic Sea[a]

Year	1994	1995	1996	1997	1998	1999	2000	2001	2002	2003	2004	2005	2006	2007	2008
Sea-air flux [kg/a]	-3702	-3760	-3493	-3713	-3915	-3647	-3646	-3643	-3568	-3483	-3610	-3703	-3477	-3905	-3992
Atmos. deposition	3536	3508	3395	3476	3450	3431	3453	3434	3416	3311	3380	3405	3321	3415	3451
Riverine inflow	1100	1100	1100	1100	1100	1100	1100	1100	1100	1100	1100	1100	1100	1100	1100
Net Hg budget	934	848	1002	863	635	903	884	891	948	928	870	802	944	601	559

[a]Negative values are fluxes from the ocean into the atmosphere and vice versa (units are kg/a).

doi: 10.12952/journal.elementa.000111.t004

4.2 Air-sea exchange in the North Sea

In the North Sea the model predicts high DEM surface concentrations at the Dutch and German coast. These are caused by the inflow of polluted water from the large rivers along the coast. The high concentrations are transported northwards along the European coast line. (Fig. 9) For the same reasons as in the Baltic Sea DEM concentrations are lowest during winter. The highest concentrations are found during spring and summer. The northern North Sea exhibits the strongest seasonal variability with the lowest concentrations during winter and the highest concentrations during summer. The high concentrations during summer in the north western North Sea are caused by increased reduction of dissolved oxidized mercury because of the inflow of phytoplankton rich water from the Atlantic. Moreover, the model estimates large DEM peaks during spring and summer in the north western North Sea and the Skaggerag which coincide with high total mercury concentrations in this area. Observations confirm these high DEM concentrations (see Section 3.1) Moreover, the model estimates a pronounced minimum in DEM concentrations during autumn in the region of the Norwegian trench and in the central North Sea north of the Dogger Bank extending towards the British coast.

Like the Baltic Sea, the North Sea is a net emitter of mercury with 5850±70 kg/a (winter 500±10, spring 800±30, summer 1750±40, autumn 2800±50) (Table 6). On average, the North Sea emits about twice as much mercury as the Baltic Sea. However, the inter-annual variability appears to be much smaller than in the Baltic Sea. The seasonal cycle is similar to the Baltic Sea, with the highest emissions during summer and autumn. During winter, the North Sea can become a sink for atmospheric mercury. Taking into account the wet deposition of around 5000 kg/a and the riverine inflow of 2500 to 2800 kg/a, the net budget for the North Sea is 1500–2000 kg/a. As a substantial amount of Hg is transported into the Atlantic ocean the North Sea can be seen as an important mercury source for the Norwegian Sea. The air-sea exchange follows the DEM concentrations as depicted in Fig. 9 with the maximum air-sea flux into the ocean occurring during winter in the northern North Sea.

Table 5. Average modelled seasonal air-sea flux of mercury [ng/m^2 day] for different Baltic Sea regions[a]

Region	Winter	Spring	Summer	Autumn	Annual	Annual
	[ng/m^2 day]	[ng/m^2 day]	[ng/m^2 day]	[ng/m^2 day]	[ng/m^2 day]	[kg/a]
Belt Sea	-24	-21	-33	-43	-30	-165 (4.5%)
Arkona Sea	-19	-16	-22	-32	-22	-270 (7.5%)
Bornholm Sea	-25	-27	-38	-55	-36	-210 (6%)
West Gotland Sea	-25	-22	-40	-52	-35	-430 (12%)
East Gotland Sea	-11	**0**	-18	-33	-16	-430 (12%)
North Gotland Sea	-5	**4**	-18	-40	-15	-110 (3%)
Bothnian Sea	-7	**-1**	-31	-36	-19	-490 (14%)
Bay of Bothnia	-22	-41	-117	-60	-60	-790 (22%)
Bay of Finland	-8	-6	-42	-54	-28	-380 (11%)
Bay of Riga	-29	-26	-49	-46	-38	-200 (5.5%)
Baltic Sea	-14	-12	-37	-43	-27	-3475

[a]Negative values are fluxes from the ocean into the atmosphere and vice versa. Archipelago and Aland Sea are included in the Bothnian Sea. The Gdansk Basin is included in the East Gotland Sea.

doi:10.12952/journal.elementa.000111.t005

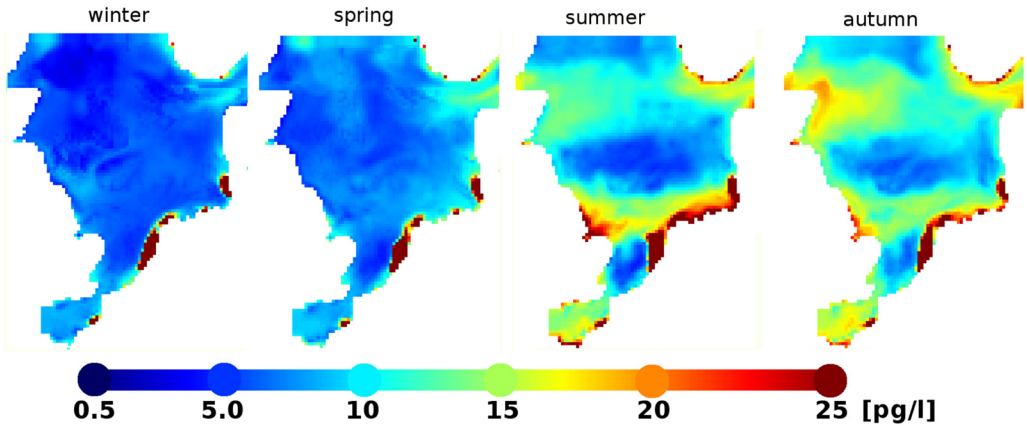

Figure 9

Modelled surface Hg^0 concentrations in the North Sea.

Seasonal average DEM concentrations in the North Sea surface layer (5m layer depth) for 1996. From left to right: winter, spring, summer, autumn.

doi: 10.12952/journal.elementa.000111.f009

4.3 Atmospheric transport

A comparison to data from EMEP stations indicates that the air-sea flux influences GEM concentrations on a regional scale during spring, summer, and autumn. On average GEM concentrations are increased by between 1% (winter) and 5% (summer) in the Baltic Sea region through coupling to the ocean model. However, for individual episodes GEM concentrations can increase more than 10% on a local scale. In regions with strong riverine mercury inflow GEM concentrations are increased significantly. Because around 50% of the mercury deposition over land is due to dry deposition of GEM, this will also influence the total mercury deposition over land. However, no observations are available to validate the impact of the emissions from the Baltic Sea on mercury dry deposition.

5. Conclusions

In this study, we coupled a regional chemistry transport model for the atmosphere (CMAQ) to a newly developed Eulerian chemistry transport model for the regional ocean (MECOSMO) to investigate the air-sea exchange of mercury in the North- and Baltic Sea. Modelled concentrations of elemental mercury in both compartments proved to be in good agreement with observations (Tables 2, 3). The calculated air-sea exchange in the Baltic Sea region was verified through comparison to observation based estimates calculated from shipborne observations. The model was able to reproduce observed surface water concentrations of dissolved elemental mercury (Figs. 2, 3, 4) and air-sea exchange in the North- and Baltic Sea (Fig. 5). Also the seasonal variability of modelled values compared reasonably with observations in the Baltic Sea (Fig. 4). Previous regional estimates of annual mercury evasions could be confirmed and the model further allowed to provide first estimates for annual mercury evasions and their variability from both seas. The modelled average annual mercury evasion into the atmosphere for the time from 1994 to 2008 is in the range of 3400–4000 kg/a for the Baltic Sea (Table 4) and 5700–6000 kg/a for the North Sea (Table 6).

The model indicates that there is a strong gradient in the air-sea flux from highly polluted coastal regions near major rivers. The largest sources are the Gotland Sea (27%), the Bay of Bothnia (22%), and the Bothnian Sea (14%) together contributing almost two thirds of the total mercury evasion from the Baltic Sea (Table 5). Moreover, the model shows a large intra annual variability of the mercury flux. During spring the northern part of the Baltic Sea can become a sink for atmospheric mercury. Also observations indicate this reversal of the flux during winter in the Bornholm and Gotland Seas (Kuss and Schneider, 2007).

Table 6. Annual total mercury fluxes for the entire North Sea[a]

Year	1994	1995	1996	1997	1998	1999	2000	2001	2002	2003	2004	2005	2006	2007	2008
Sea-air flux [kg/a]	-5898	-5852	-5876	-5766	-6007	-5855	-5832	-5733	-5824	-5713	-5915	-5802	-5880	-5894	-5917
Atmos. deposition	5094	5078	5062	5045	5029	5013	4997	4998	4980	4971	4962	4954	4945	4936	4927
Riverine inflow	2507	2507	2507	2507	2507	2507	2507	2507	2507	2507	2507	2760	2837	2837	2837
Net Hg budget	1703	1733	1693	1786	1529	1665	1672	1772	1663	1765	1554	1912	1902	1879	1847

[a]Negative values are fluxes from the ocean into the atmosphere and vice versa (units are kg/a).

doi: 10.12952/journal.elementa.000111.t006

Investigating the seasonal cycle of mercury evasion from the Baltic, the model indicates a minimum during spring and winter time, which is due to lower dissolved elemental mercury (DEM) concentrations in the ocean and higher gaseous elemental mercury concentrations (GEM) in the atmosphere. The GEM concentrations are increased because of higher emissions from coal fired power plants and a lower planetary boundary layer. Because of the much smaller gradient during winter, the high wind speeds in this season have no significant effect of the air-sea exchange. During summer and autumn the air-sea exchange is mainly driven by high DEM concentrations in the ocean which are caused by the high biological activity and the connected bio-reduction of dissolved oxidized mercury. During autumn higher wind speeds increase the air-sea flux leading to the highest seasonal net mercury evasion for the whole Baltic Sea. The seasonal cycle in the North Sea is similar to the Baltic Sea. During winter the northern part of the North Sea can become a sink for atmospheric mercury.

A comparison of average DEM concentrations and air-sea fluxes for the Bornholm and Gotland Sea indicate that the model could be missing local DEM peaks during summer. It is expected, that the observed peaks are linked to biological activity. Indeed, the model does exhibit DEM peaks, and peaks in air-sea flux, correlated to primary production (Fig. 3). It cannot be verified whether the observations coincide with such a spatially and locally temporal peak in primary production or whether the model tends to underestimates DEM concentrations in this region. Additional observations would be necessary and more detailed model sensitivity studies in the future could increase the insights into the marine cycling of DEM and help to resolve this question.

Taking into account wet deposition and riverine inflow of Hg, the model predicts an annual net mercury budget of 500–1000 kg/a for the Baltic Sea. For the North Sea the model calculates an annual net Hg budget between 1500 and 2500 kg/a. As there is only limited permanent sedimentation in the North Sea, these results indicate that the North Sea is an important Hg source for the Norwegian Sea.

Finally, we investigated the impact of mercury emissions from the North- and Baltic Sea on atmospheric transport of GEM. A comparison of downwind EMEP stations showed that the model performance improves when including these emissions. Directly at the German coast, GEM concentrations are increased by up to 10%. Moreover, GEM peaks with a duration of up to a few days could be attributed to air-sea exchange from the Baltic. In a vicinity of 100 km to 200km the annual effect is reduced to 1%–4%. However, at individual days, depending on atmospheric conditions, GEM evasion from the Baltic Sea can still have large impacts even on a regional scale.

Appendix A

P_i = Predicted value from Model

O_i = Observed value

N = sample size

Mean

$$\bar{O} = \frac{1}{N}\sum_{i=1}^{N} O_i \bar{P} = \frac{1}{N}\sum_{i=1}^{N} P_i \quad \text{(A1)}$$

Normalized Mean Bias (NMB)

$$NMB = \frac{\bar{P} - \bar{O}}{\bar{O}} \quad \text{(A2)}$$

Mean Normalized Bias (MNB)

$$MNB = \frac{1}{N}\sum_{i=1}^{N}\left(\frac{P_i - O_i}{O_i}\right) \quad \text{(A3)}$$

Mean Normalized Error (MNE)

$$MNE = \frac{1}{N}\sum_{i=1}^{N}\left(\frac{|P_i - O_i|}{O_i}\right) \quad \text{(A4)}$$

References

Amos HM, Jacob DJ, Streets DG, Sunderland EM. 2013. Legacy impacts of all-time anthropogenic emissions on the global mercury cycle. *Global Biogeochem Cy* **27**: 1–12. doi: 10.1002/gbc.20040.

Andersson ME, Gaerdfeldt K, Wängberg I, Stroemberg D. 2008. Determination of Henriy's law constant for elemental mercury. *Chemosphere* **73**: 587–592.

Baeyens W, Leermakers M. 1998. Elemental mercury concentrations and formation rates in the Scheldt estuary and the North Sea. *Mar Chem* **60**(3–4): 257–266.

Barthel K, Daewel U, Pushpadas D, Schrum C, Arthun M, et al. 2012. Resolving frontal structures: On the computational costs and pay-off using a less diffusive but computational more expensive advection scheme. *Ocean Dynamics*. doi: 10.1007/s10236-012-0578-9.

Bash JO. 2010. Description and initial simulation of a dynamic bidirectional air-surface exchange model for mercury in Community Multiscale Air Quality (CMAQ) model. *J Geophys Res* **115** (D6): D06305.

Beldowski J, Pempkowiak J. 2003. Horizontal and vertical variabilities of mercury concentration and speciation in sediments of the Gdansk Basin, Southern Baltic Sea. *Chemosphere* **5**(3): 645–654.

Bieser J, Aulinger A, Matthias V, Quante M, Builtjes P. 2011a. SMOKE for Europe – adaptation, modification and evaluation of a comprehensive emission model for Europe. *Geosci Model Dev* **4**: 47–68. doi: 10.5194/gmd-4-47-2011.

Bieser J, Aulinger A, Matthias V, Quante M, Denier van der Gon HAC. 2011b. Vertical emission profiles for Europe based on plume rise calculations. *Environ Pollut* **159**: 2935–2946. doi: 10.1016/j.envpol.2011.04.030.

Bieser J, DeSimone F, Gencarelli C, Geyer B, Hedgecock IM, et al. 2014. A diagnostic evaluation of modelled mercury wet depositions in Europe using atmospheric speciated high-resolution observations. *Environ Sci Pollut R* **21**(16). doi: 10.1007/s11356-014-2863-2.

Borg H, Jonsson P. 1995. Large-Scale Metal Distribution in Baltic Sea Sediments. *Marine Pollution Bulletin* **32**(1): 8–12.

Brigham ME, Wentz DA, Aiken GR, Krabbenhoft DP. 2009. Mercury cycling in stream ecosystems. 1. Water column chemistry and transport. *Environ Sci Technol* **43**: 2720–2725.

Bullock OR, Atkinson D, Braverman T, Civolo K, Dastoot A, et al. 2008. The North American Mercury Model Intercomparison Study (NAMMIS): Study description and model-to-model comparisons. *J Geophys Res-Atmos* **133**(D17).

Bullock OR, Brehme KA. 2002. Atmospheric mercury simulations using the CMAQ model: Formulation description and analysis of wet deposition results. *Atmos Environ* **36**: 2135–2146.

Byun DW, Ching JKS. 1999. Science Algorithms of the EPA Models-3 Community Multi-scale Air Quality (CMAQ) Modeling System. *EPA/600/R-99/030*. US EPA National Exposure Research Laboratory. Research Triangle Park, NC.

Byun DW, Schere KL. 2006. Review of the governing equations, computational algorithms, and other components of the Models-3 Community Multiscale Air Quality (CMAQ) modeling system. *Applied Mechanics Reviews* **59**(2): 51–77.

Coquery M, Cossa D. 1992. The distribution of mercury species in the Seine Estuary, France. *Intern. Conf. On Mercury as a Global Pollutant*. 31 May – 04 June 1992.

Coquery M, Cossa D. 1995. Mercury speciation in surface waters of the North Sea. *Neth J Sea Res* **34**: 245–257.

Daewel U, Schrum C. 2013. Simulating long-term dynamics of the coupled North Sea and Baltic Sea ecosystem with ECOSMO II. Model description and validation. *J Mar Sys* **119–120**: 30–49. doi: 10.1016/j.jmarsys.2013.03.008.

Doms G. 2011. A Description of the Nonhydrostatic Regional COSMO model. Part I: Dynamics and Numerics. *Tech. rep., Deutscher Wetterdienst*. http://www.cosmo-model. org/content/model/documentation/core/cosmoDyncsNumcs.pdf. Accessed 8 April 2015.

Doms G, Förstner J, Heise E, Herzog H-J, Mrionow D, et al. 2011. A Description of the Nonhydrostatic Regional COSMO Model. Part II: Physical Parameterization. *Tech. rep., Deutscher Wetterdienst*. http://www.cosmo-model.org/content/model/documentation/core/cosmoPhysParamtr.pdf. Accessed 8 April 2015.

ECE (Economic Commission for Europe). 2010. Hemispheric Transport of Air Pollution. Part-B: Mercury. New York and Geneva: United Nations. Pirrone N, Keating T, eds.

Garfeldt K, Feng X, Sommar J, Lindqvist O. 2001. Total gaseous mercury exchange between air and water at river and sea surfaces in Swedish coastal regions. *Atmos Environ* **35**: 3027–3038.

Geyer B. 2014. High-resolution atmospheric reconstruction for Europe 1948–2012: coastDat2. *Earth Syst Sci Data* **6**: 147–164. doi: 10.5194/essd-6-147-2014.

Green NW, Heldal HE, Måge A, Aas W, Gafvert T, et al. 2011. Tilførselsprogrammet 2010. Overvåking av tilførsler og miljøtilstand i Nordsjøen. *NIVA rapport 6187-2011*. Klima-og forurensningsdirektoratet (Klif), Rapport TA 2810/2011. ISBN 978-82-577-577-5992-3: IPCS 1992.

HELCOM. 2007. Heavy Metal Pollution to the Baltic Sea in 2004. *Baltic Sea Environment Proceedings. No. 108*: 33 pp.

HELCOM. 2011. Fifth Baltic Sea Pollution Load Compilation. *Baltic Sea Environment Proceedings No. 128*: 56 pp.

Heyes A, Mason RP, Kim E-H, Sunderland E. 2006. Mercury methylation in estuaries: Insights from using measuring rates using stable mercury isotopes. *Mar Chem* **102**(1–2): 134–147. doi: 10.1016/j.marchem.2005.09.018.

Horowitz HM, Jacob DJ, Amos HM, Streets DG, Sunderland EM. 2014. Historical mercury releases from commercial products: Global environmental implications. *Environ Sci Technol* **48**(17): 10242–10250.

Houyoux MR, Vukovich JM, Coats Jr CJ, et al. 2000. Emission inventory development and processing for the Seasonal Model for Regional Air Quality (SMRAQ) project. *J Geophys Res* **105**(D7): 9079–9090.

Huijnen V, Williams J, van Weele M, van Noije T, Krol M, et al. 2010. The global chemistry transport model TM5: Description and evaluation of the tropospheric chemistry version 3.0. *Geosci Model Dev* **3**: 445–473. doi: 10.5194/gmd-3-445-2010.

Janssen F, Schrum C, Backhaus J. 1999. A climatological dataset of temperature and salinity for the North Sea and the Baltic Sea. *Deutsche Hydrographische Zeitschrift, 9, 1999*, ISSN 0946-2015.

Kalnay E, Kanamitsu M, Kistler R, Collins W, Deaven D, et al. 1996. The NCEP/NCAR 40-year reanalysis project. *B Am Meteorol Soc* **77**: 437–471.

Kersten M, Dicke M, Kriews M, Naumann K, Schmidt D, et al. 1988. Distribution and Fate of Heavy Metals in the North Sea, in, Bayne BL, Duursma EK, Förstner U, eds., *Pollution of the North Sea*. Springer: Berlin Heidelberg. doi: 10.1007/978-3-642-73709-1_19.

Kuss J, Schneider B. 2007. Variability of the Gaseous Elemental Mercury Sea-Air Flux of the Baltic Sea. *Environ Sci Technol* **41**: 8018–8023.

Kuss J. 2014. Water-air gas exchange of elemental mercury: An experimentally determined mercury diffusion coefficient for Hg^0 water-air flux calculations. *Limnol Oceanogr* **59**(5): 1461–1467. doi: 10.4319/lo.2014.59.5.1461.

Kuss J, Wasmund N, Nausch G, Labrenz M. 2015. Mercury Emission by the Baltic Sea: A Consequence of Cyanobacterial Activity, Photochemistry, and Low-Light Mercury Transformation. *Environ Sci Technol* **49**(19). doi: 10.1021/acs.est.5b02204.

Leermakers M, Galletti S, De Galan S, Brion N, Baeyens W. 2001. Mercury in the Southern North Sea and Scheldt estuary. *Mar Chem* **75**: 229–248.

Lehnherr I. St. Louis VL, Hintelmann H, Kirk JL. 2011. Methylation of inorganic mercury in polar marine waters. *Nat Geosci* **3**:298–302.

Mason RP, Reinfelder JR, Morel FM. 1996. Uptake, Toxicity, and Trophic Transfer of Mercury in a Coastal Diatom. *Environ Sci Technol* **30**: 1835–1845.

Matthias V, Quante M, Aulinger A. 2009. Determination of the optimum MM5 configuration for long term CMAQ simulations of aerosol bound pollutants in Europe. *Environ Fluid Mech* **9**: 91–108. doi: 10.1007/s10652-008-9103-6.

Monperrus M, Tessier E, Amouroux D, Leynaert A, Huonnic P, et al. 2007. Mercury methylation, demethylation and reduction rates in coastal and marine surface waters of the Mediterranean Sea. *Mar Chem* **107**(1): 49–63. doi: 10.1016/j.marchem.2007.01.018.

Nightingale PD, Malin G, Law CS, Watson AJ, Liss PS, et al. 2000. In-situ evaluation of air-sea gas exchange parameterizations using novel conservative and volatile tracers. *Global Biogeochem Cy* **14**: 373–387.

Pacyna EG, Pacyna JM, Fudala J, Strzelecka-Jastrab E, Hlawiczka S, et al. 2006a. Mercury emissions to the atmosphere from anthropogenic sources in Europe in 2000 and their scenarios until 2020. *Sci Tot Env* **370**(1): 147–156. doi: 10.1016/j.scitotenv.2006.06.023.

Pacyna EG, Pacyna JM, Steenhuisen F, Wilson S. 2006b. Global anthropogenic mercury emission inventory for 2000. *Atmos Environ* **40**(22): 4048–4063. doi: 10.1016/j.atmosenv.2006.03.041.

Pacyna JM, Pacyna EG, Steenhuisen F, Wilson S. 2003. Mapping 1995 global anthropogenic emissions of mercury. *Atmos Environ* **37**(1):109–117. doi: 10.1016/S-1352-2310(03)00239-5.

Pempkowiak J, Cossa D, Sikora A, Sanjuan J. 1998. Mercury in water and sediments of the southern Baltic Sea. *Sci Total Environ* **213**(1–3): 185–192.

Pierce T, Geron C, Pouliot G, Kinnee E, Vukovich J. 2002. Integration of the Biogenic Emissions Inventory System (BEIS3) into the Community Multiscale Air Quality (CMAQ) Modeling System. *Proceedings of the AMS 4th Urban Environment Symposium. May 20–23, 2002*. Norfolk, Virginia. ams.confex.com/ams/AFMAPUE/12AirPoll/abstracts/37962.htm.

Pirrone N, Cinnirella S, Feng X, Finkelman RB, Friedli HR, et al. 2010. Global mercury emissions to the atmosphere from anthropogenic and natural sources. *Atmos Chem Phys* **10**(13): 5951–5964.

Qureshi A, O'Driscoll NJ, MacLeod M, Neuhold Y-M, Hungerbühler K. 2010. Photoreactions of mercury in surface ocean water, gross reaction kinetics and possible pathways. *Environ Sci Technol* **44**:644–649.

Qureshi A. 2011. Quantifying and Reducing Uncertainties in Global Mercury Cycling. *Disseration ETH No. 19709*. Zürich, Switzerland.

Ranchou-Peyruse M, Monperrus M, Bridou R, Duran R, Amouroux D, et al. 2009. Overview of Mercury Methylation Capacities among Anaerobic Bacteria Including Representatives of the Sulphate-Reducers: Implications for Environmental Studies. *Geomicrobiology* **26**(1). doi: 10.1080/01490450802599227.

Ritter B, Geleyn JF. 1992. A comprehensive radiation scheme for numerical weather prediction models with potential applications in climate simulations. *Mon Weather Rev* **120**: 303–325. doi: 10.1175/1520-0493.

Rockel B, Will A, Hense A. 2008. The Regional Climate Model COSMO-CLM (CCLM). *Meteorol Z* **17**: 347–248.

Sarwar G, Luecken D, Yarwood G. 2007. Chapter 2.9 Developing and implementing an updated chlorine chemistry into the community multiscale air quality model. *Developments in Environmental Science* **6**: 168–176. doi: 10.1016/S1474-8177(07)06029-9.

Schaettler U, Doms G, Schraff C. 2008. A Description of the Nonhydrostatic Regional COSMO-Model Part VII: User's Guide. *Tech. Rep., Deutscher Wetterdienst*.

Schartup AT, Ndu U, Mason RP, Sunderland EM. 2015. Contrasting effects of marine and terrestrially derived dissolved organic matter on mercury speciation and bioavailability in seawater. *Environ Sci Technol*. doi: 10.1021/es506274x.

Schrodin R, Heise E. 2001. The multi-layer-version of the DWD soil model TERRA/LM, Tech. Rep, Consortium for Small-Scale Modelling (COSMO). http: //www.cosmo-model.org/content/model/documentation/techReports/docs/techReport02.pdf. Accessed 8 April 2015.

Schrum C, Alekseeva I, St. John M. 2006. Development of a coupled physical–biological ecosystem model ECOSMO Part I: Model description and validation for the North Sea. *J Mar Sys*. doi: 10.1016/j.jmarsys.2006.01.005.

Schrum C, Backhaus JO. 1999. Sensitivity of atmosphere-ocean heat exchange and heat content in the North Sea and the Baltic Sea. *Tellus A* **51**(4): 526–549. doi: 10.1034/j.1600-0870.1992.00006.x.

Schwede D, Pouliot G, Pierce T. 2005. Changes to the Biogenic Emissions Inventory System Version 3 (BEIS3). *Proceedings of the 4th CMAS Models-3 Users' Conference 26–28 September 2005*. Chapel Hill, NC. www.cmascenter.org/conference/2005/abstracts/2_7.pdf.

Seifert A, Beheng KD. 2001. A double-moment parameterization for simulating autoconversion, accretion and self-collection. *Atmos Res* **59–60**:265–281. doi: 10.1016/S0169-8095(01)00126-0.

Seifert A, Beheng KD. 2006. A two-moment cloud microphysics parameterization for mixed-phase clouds. Part 1: Model description. *Meteorol Atmos Phys* **92**:45–66.

Soerensen A, Sunderland EM, Holmes CD, Jacob DJ, Yantosca RM, et al. 2010. An Improved Global Model for Air-Sea Exchange of Mercury: High Concentrations over the North Atlantic. *Environ Sci Technol* **44**: 8574–8580.

Sonke JE, Heimbürger L-E, Dommergue A. 2013. Mercury biogeochemistry: Paradigm shifts, outstanding issues, and research needs. *Comptes Rendus Geoscience* **345**(5–6): 213–224. doi: 10.1016/j.crte.2013.05.002.

Steppeler J, Doms G, Schattler U, Bitzer HW, Gassmann A, et al. 2003. Meso-gamma scale forecasts using the nonhydrostatic model LM. *Meteorol Atmos Phys* **82**: 75–96. doi: 10.1007/s00703-001-0592-9.

Strode SA, Jaegle L, Selin N, Jacob D, Park R, et al. 2007. Air-sea exchange in the global mercury cycle. *Global Biogeochem Cy* **21**. doi: 10.1029/2006 GB002766.

Tanaka PL, Allen DT, McDonald-Buller EC, Chang S, Kimura Y, et al. 2003. Development of a chlorine mechanism for use in the carbon bond IV chemistry model. *J Geophys Res-Atmos* **108**. doi: 10.1029/2002JD002432.

Tiedtke M. 1989. A comprehensive mass flux scheme for cumulus parameterization in large-scale models. *Mon Weather Rev* **117**: 1779–1800. doi: 10.1175/1520-0493(1989)117.

Travnikov O, Ilyin I. 2009. The EMEP/MSC-E mercury modeling system, in Pirrone N, Mason RP, eds., *Mercury Fate and Transport in the Global Atmosphere*. Dordecht: Springer: pp. 571–587.

UNC Carolina Environmental Program. 2005. Sparse Matrix Operator Kernel Emissions (SMOKE) Modeling System. North Carolina, USA: UNC Chapel Hill.

UNEP (United Nations Environment Program). 2013a. Mercury: Time to act. *Tech. Rep., Chemicals Branch, Division of Technology, Industry and Economics, United Nations Environment Programme (UNEP)*.

UNEP (United Nations Environmental Program). 2013b. Minamata Convention on Mercury, Text and Annexes. http://www.mercuryconvention.org/Portals/11/documents/Booklets/Minamata%20Convention%20on%20Mercury_booklet_English.pdf.

UNEP (United Nations Environment Program). 2013c. Global Mercury Report. Geneva, Switzerland: UNEP.

Vukovich J, Pierce T. 2002. The Implementation of BEIS3 within the SMOKE Modeling Framework. *Proceedings of the 11th International Emissions Inventory Conference*. Atlanta, Georgia. April 15-18, 2002. www.epa.gov/ttn/chief/conference/ei11/modeling/vukovich.pdf.

Wängberg I, Schmolke S, Schager P, Munthe J, Ebinghaus R, et al. 2001. Estimates of air-sea exchange of mercury in the Baltic Sea. *Atmos Environ* **35**(2001): 5477–5484.

Wanninkhof R. 1992. Relationship between windspeed and gas exchange over the ocean. *J Geophys Res* **97**: 7373–7382.

Weigelt A, Slemr F, Bieser J, Ebinghaus R, Eposito G, et al. Observations based emission speciation from a modern coal fired power plant in central Europe. In preparation.

Weiss A, Kuss J, Peters G, Schneider B. 2007. Evaluating transfer velocity-wind speed relationship using a long term series of direct eddy correlation CO2 flux measurements. *J Mar Sys* **66**:130–139.

Whitten GZ, Heo G, Kimura Y, McDonald-Buller E, Allen DT, et al. 2010. A new condensed toluene mechanism for Carbon Bond: CB05-TU. *Atmos Environ* **44**: 5346–5355.

Wilson S, Munthe J, Sundseth K, Kindbom K, Maxson P, et al. 2010. Updating Historical Global Inventories of Anthropogenic Mercury Emissions to Air. *Arctic Monitoring and Assessment Programme (AMAP) Technical Report No. 3*. Oslo, Norway: AMAP Secretariat.

Wurl O, Elsholz O, Ebinghaus R. 2001. On-line determination of total mercury in the Baltic Sea. *Analytica Chimica Acta* **438**: 245–249.

Yarwood G, Rao S, Yocke M, Whitten GZ. 2005. Updates to the Carbon Bond Mechanism: CB05. *Report to the U.S. Environmental Protection Agency. RT-04-00675*. http://www.camx.com/publ/pdfs/.

Zhijia C, Zhang X, Wang Z. 2011. Elemental mercury in coastal seawater of Yellow Sea, China: Temporal variation and air-sea exchange. *Atmos Environ* **45**: 183–190.

Contributions

- Substantial contributions to conception and design: JB, CS
- Acquisition of data: JB, CS
- Analysis and interpretation of data: JB
- Drafting the article or revising it critically for important intellectual content: JB, CS
- Final approval of the version to be published: JB, CS

Acknowledgments

We want to thank those supporting this work with observational data: John Munthe, Ingvar Wängberg, Elke Bieber, Andreas Weigelt, Hans-Herbert Kock and Ralf Ebinghaus for atmospheric GEM observations as well as Joachim Kuss, Ingvar Wängberg, Oliver Wurl, and Ralf Ebinghaus for dissolved gaseous mercury observations in the North- and Baltic Sea. Special thanks go to Joachim Kuss who shared the raw data for four cruises in the Baltic Sea performed in 2006 which were invaluable for the model evaluation and helped us to interpret to model results. Moreover, we obtained mercury observations and river load data collected, reported and further distributed by HELCOM, OSPAR, ICES, and EMEP. We thank our colleagues providing input data for the regional models: Twan van Noije for TM5 model data, Oleg Travnikov for data on atmospheric mercury concentrations from the GLEMOS model, Beate Geyer for COSMO-CLM meteorological data, and AMAP (Simon Wilson and Fritz Steenhuisen) and Josef Pacyna for historic mercury emission datasets. US EPA is gratefully acknowledged for the use of CMAQ and SMOKE. Corinna Schrum thanks the Meltzer Research fund of the University of Bergen, Norway for support of her sabbatical, which enabled this research project. Finally, we want to thank Anne Soerensen and Katarina Garfeldt for their support during the publication process which substantially improved this paper.

Funding information

This study received financial support from the FP7 GMOS project (No. 265113) and from the Norwegian Research Council through EU-FP7 SeasERA project SEAMAN (NRC-227779/E40).

Competing interests

We are not aware of any competing interests.

Data accessibility statement

For access to the model data, contact johannes.bieser@hzg.de.